Lawrence Berkeley National Laboratory

Title
New capabilities for modeling intense beams in heavy ion fusion drivers

Permalink
https://escholarship.org/uc/item/3tz5h0j7

Authors
Friedman, A.
Barnard, J.J.
Bieniosek, F.M.
et al.

Publication Date
2003-09-01

NEW CAPABILITIES FOR MODELING INTENSE BEAMS IN HEAVY ION FUSION DRIVERS

A. Friedman,[1,2*] J. J. Barnard,[1,2] F. M. Bieniosek,[1,3] C. M. Celata,[1,3] R. H. Cohen,[1,2]
R. C. Davidson,[1,4] D. P. Grote,[1,2] I. Haber,[5] E. Henestroza,[1,3] E. P. Lee,[1,3]
S. M. Lund,[1,2] H. Qin,[1,4] W. M. Sharp,[1,2] E. Startsev,[1,4] and J-L. Vay[1,3]

[1]Heavy Ion Fusion Virtual National Laboratory
[2]Lawrence Livermore National Laboratory, Livermore CA USA
[3]Lawrence Berkeley National Laboratory, Berkeley CA USA
[4]Princeton Plasma Physics Laboratory, Princeton NJ USA
[5]University of Maryland, College Park MD USA

Significant advances have been made in modeling the intense beams of heavy-ion beam-driven Inertial Fusion Energy (Heavy Ion Fusion). In this paper, a roadmap for a validated, predictive driver simulation capability, building on improved codes and experimental diagnostics, is presented, as are examples of progress. The Mesh Refinement and Particle-in-Cell methods were integrated in the WARP code; this capability supported an injector experiment that determined the achievable current rise time, in good agreement with calculations. In a complementary effort, a new injector approach based on the merging of ~100 small beamlets was simulated, its basic feasibility established, and an experimental test designed. Time-dependent 3D simulations of the High Current Experiment (HCX) were performed, yielding voltage waveforms for an upcoming study of bunch-end control. Studies of collective beam modes which must be taken into account in driver designs were carried out. The value of using experimental data to tomographically "synthesize" a 4D beam particle distribution and so initialize a simulation was established; this work motivated further development of new diagnostics which yield 3D projections of the beam phase space. Other developments, including improved modeling of ion beam focusing and transport through the fusion chamber environment and onto the target, and of stray electrons and their effects on ion beams, are briefly noted.

I. INTRODUCTION

A key goal of the Heavy Ion Fusion (HIF) program is a well benchmarked, integrated source-to-target simulation capability that can be used to support the design and inter-

pretation of experiments, and facilitate the design of future facilities. This paper describes progress toward this goal, emphasizing beam modeling for the driver accelerator.
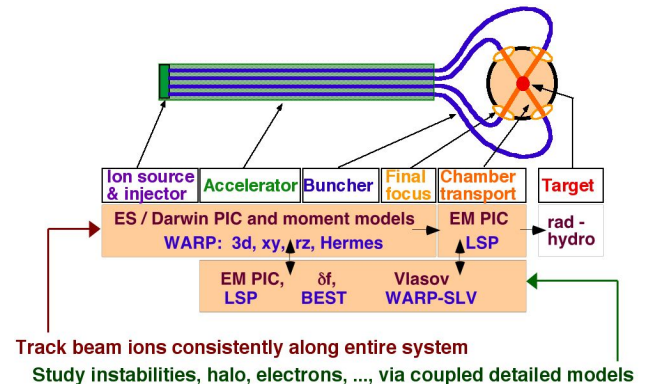

Figure 1: A depiction of the strategy being pursued for consistent, detailed end-to-end beam simulation.

The Heavy Ion Fusion beam research program [1, 2, 3] employs a suite of simulation codes; see Fig. 1 for a roadmap. For studies of beams in the driver accelerator, drift-compression line, and final-focusing optical system, the principal tool is a particle-in-cell (PIC) code known as WARP [4] (named for the "warped" coordinates it uses for a bent beam line). In the fusion chamber, the principal tool is the hybrid implicit electromagnetic PIC code LSP [5] ("Large Scale Plasmas"). BEST [6] ("Beam Equilibrium, Stability, and Transport"), a nonlinear perturbative particle code with minimal statistical "noise," is the principal tool for studies of plasma modes on the beams. Hermes and Circe are moment-based models in WARP which are useful for rapid iterative design. The Semi-Lagrangian Vlasov

method [7] solves the Vlasov equation by advancing the phase space density on a grid; a prototype package (SLV) in WARP using the method will be well-suited for studies of low-density beam halo (which must be kept minimal).

For high-fidelity simulations of planned experiments, it is important to follow beams self-consistently, because they have a "long memory" of forces imposed on them. To accomplish this, beam data must be passed from WARP, to LSP, to the target physics radiation-hydrodynamics code [8]. In addition, linkage from this "main sequence" into other calculations that treat specific sections of the system, *e.g.* with more detailed physics models or higher resolution, enable those detailed studies to simulate the "right beam." This strategy is indicated in Fig. 1. To date, the link from WARP to LSP has been exercised most extensively.

In Section II below, we describe use of mesh refinement with the particle-in-cell method to facilitate simulations of injector diodes, and present a simulation of an experiment on the Source Test Stand (STS500) [9] that is exploring the rapidity with which the beam current may be made to rise. In Section III we present a 3D time-dependent simulation of the High Current Experiment (HCX) [10] that yielded the voltage waveform that will correct the initial space-charge-driven energy variation of the beam head. In Section IV we describe recent simulations of collective beam modes using BEST [6]. In Section V we discuss the use of experimental diagnostics to tomographically "synthesize" a good approximation to the beam's 4D transverse phase space density [11, 12]. Finally, in Section VI we briefly outline other developments in HIF beam simulation.

II. MESH REFINEMENT; INJECTOR SIMULATION

WARP has recently been enhanced with Mesh Refinement (MR) capabilities that concentrate grid information where spatial resolution is most needed.[13] The method has been implemented directly into the axisymmetric (r,z) package, and is enabling, for the first time, numerically converged studies of time-dependent space-charge-limited flows in real geometries. WARPs 3D package is currently being integrated with the Adaptive MR (AMR) solver Chombo [14] developed by the NERSC computer center. (In AMR, the mesh evolves as the simulation progresses.)

Simulations using MR-PIC are revealing the detailed phase space of beams as they are injected, and confirming that it should be possible to launch a beam with a short current rise time, as needed for some concepts of a near-term integrated experiment. Minimization of the required volt-seconds is an important way to reduce costs; for many purposes a short-pulse integrated experiment would be advantageous, provided the beam head and tail can be kept sufficiently short. To explore this physics, the STS-500 test stand at LLNL was run at a reduced voltage of ~20 kV, so that the voltage rise time of the existing pulser matched

a numerically-optimized value.[9] In contrast with the behavior "traditionally" observed in ion diodes, the current pulse exhibited only minimal overshoot, in good agreement with the simulations (which used the applied voltage measured from STS500). Obtaining numerically-converged results required that the mesh be refined by a factor of a thousand in the vicinity of the source, and to a lesser degree at the beam edge. Panel (a) of Fig. 2 shows a side-on view of the simulated beam once it has reached steady state, along with the diode and Faraday cup; shading denotes beam density. Panel (b) shows the as-measured (lower curve) and simulated (upper curve) Faraday cup signals, including ion and induced (image) contributions. Subtracting the induced current from both traces (panel c) shows that the ion pulse indeed has a faster rise (~300 ns) than the Faraday cup signal. Further runs showed that with an optimized waveform the rise can be further shortened, especially near the top. This research indicates that a diode running at 500 kV with a suitably fast voltage rise and optimized waveform should yield a current rise faster than 50 ns.
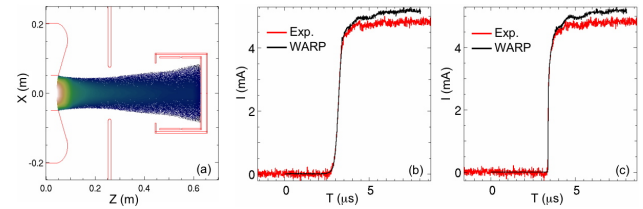

Figure 2: Simulation of STS500 diode tested at reduced voltage to study physics of rapid current rise (see text)

In a complementary effort, simulations have demonstrated the basic feasibility of the novel "merging beamlets" approach to a compact injector; an initial optimization has been carried out.[15] Here, the issue is dilution of the beam phase space (emittance growth) during merging. The simulations showed that the emittance from an optimized system should be similar to that obtainable from the large-diameter source approach, encouraging further development of the multibeamlet approach. Frames from a WARPxy (transverse-slice) movie are shown in Fig. 3.
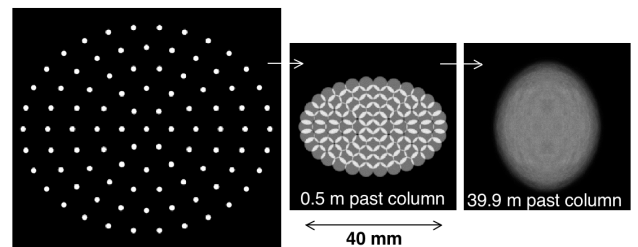

Figure 3: A sequence of "snapshots" of merging beamlets, as computed using a high-resolution WARPxy simulation.

That simulation followed 91 beamlets (each 0.006 A, with emittance 0.003 π-mm-mr), accelerated as they merge through from 1.2 to 1.6 MeV; 29 M particles, a 1024×1024 grid, and 4000 time steps were used, requiring 18.2 hours on 64 processors of the NERSC IBM SP computer.

III. 3D TIME-DEPENDENT HCX SIMULATIONS

If the pulse rise time is insufficiently rapid, the beam head can be "mismatched" to the transport channel, and can expand enough to result in particle loss. Such behavior can indeed be seen in the WARP3d simulation of the HCX injector as currently configured, as shown in the large image in Fig. 4. A future upgrade will reduce the rise time of the gate voltage that switches on the beam, and other WARP simulations have confirmed that the beam head does not scrape under those circumstances.

New 3D simulations of HCX through the end of the matching section have shed light on the longitudinal beam phase space and the voltage waveforms needed to "catch" the beam and control its head; to this end, experiments testing a pulser developed by First Point Scientific, Inc., are planned for the coming year.[16] The inset at lower left of Fig. 4 is a time-history of the mean energy of the beam particles in the simulation, as they pass the plane where the first so-called "ear" pulse will be applied.
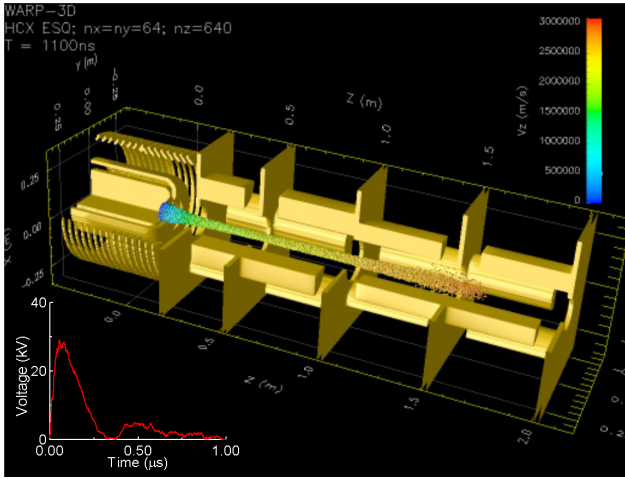

Figure 4: Depiction of the beam head passing through the HCX injector, in a time-dependent WARP3d simulation; inset: derived induction pulser voltage waveform required at exit of matching section for beam-end control.

IV. SIMULATIONS OF COLLECTIVE PROCESSES

The low-noise, three-dimensional nonlinear perturbative (δf) particle simulation scheme in BEST [6] is facilitating study of the collective stability and transport properties of intense charged particle beams. In the absence of

background electrons and temperature anisotropy, BEST simulations have demonstrated stable beam propagation over thousands of meters [17]. In the presence of an overly large quantity of background electrons, however, large-scale parallel simulations show that the interaction between the beam ions and background electrons can result in a strong two-stream instability, leading to a dipole transverse displacement of the beam ions and background electrons [18]. Typical simulations of the two-stream instability employ 10^6 simulation particles for 5×10^{11} particle-time steps on 128 processors of the NERSC IBM SP computer.

In beams with strongly anisotropic distributions (unequal temperatures transverse and parallel to the direction of mean motion) $T_{\perp b} \gg T_{\parallel b}$, it has been known for some time that a collective instability can develop [19, 20] if there is sufficient coupling between the transverse and longitudinal degrees of freedom; the mode is similar to the well-know Harris instability in unbounded magetoplasma [21]. Furthermore, as a result of transverse emittance growth and "kinematic" longitudinal cooling (due to acceleration at fixed pulse duration) in certain sections of accelerator systems, such anisotropies can arise naturally. Recently, BEST was used [22, 23, 24] to study the stability properties of intense nonneutral charged particle beams with such temperature anisotropy. The most unstable modes were identified and their eigenfrequencies and radial mode structure determined. The dependence of the mode on beam intensity, its nonlinear saturation properties, and the effects of the instability on beam emittance are also being explored. Simulation results show that moderately intense beams with $s_b = \omega_{pb}^2/2\gamma_b^2\omega_{\beta\perp}^2 \gtrsim 0.5$ ($\omega_{\beta\perp}$ is the smooth-focusing frequency) are linearly unstable to short-wavelength perturbations with $k_z^2 r_b^2 \gtrsim 1$, provided the ratio of longitudinal to transverse temperatures is smaller than some threshold value. The left panel of Fig. 5 shows the
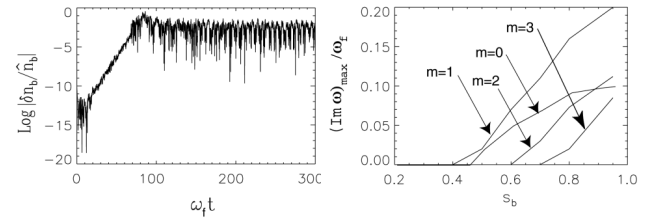

Figure 5: Studies of the anisotropy-driven beam mode using BEST. Left panel: growth and saturation; right panel: parametric dependence of growth rate.

linear growth and nonlinear saturation of the mode, illustrating the ability of the δf technique to follow both small-signal and saturated oscillations. The right panel shows the variation of the growth rate with beam density and azimuthal mode number. In the nonlinear saturation stage, the total distribution function is still far from equipartitioned;

nonetheless, the transfer of thermal energy from transverse to longitudinal motions is significant, and the possibility of such longitudinal heating represents a constraint which must be taken into consideration in HIF driver design optimization. We are currently looking for signatures of the instability developing from the source in WARP simulations of present-day and near-term experiments.

V. 4D TOMOGRAPHY & OPTICAL DIAGNOSTICS

In present-day experiments, a variety of diagnostics yield information on the beam particle distribution function. Good shot-to-shot reproducibility enables the acquisition of detailed 2D projections of the beam's 4D transverse particle distribution function $f(x, y, x' \equiv p_x/p_z, y' \equiv p_y/p_z)$ at a sequence of stations, using moving slits and Faraday cups. These projections do not uniquely specify the 4D distribution, so we use maximum-entropy Monte-Carlo techniques to complete the specification and tomographically "synthesize" an approximation to f.

In order to to assess the potential utility of launching simulations using experimental data, we began with a self-consistent "transverse slice" WARPxy simulation of HCX beginning at the source, for which the true 4D distribution was known. Input to the syntheses consisted of projectional phase-space densities (obtained as moments of the simulated particles from the reference run at the entrance to the HCX transport line) in the (x, x') and (y, y') planes, and, for the 3-plane synthesis, also the (x, y) plane. Fig. 6 compares the emittance evolution in runs with various initial particle distributions [25]; all begin at the injector exit ($z= -3.11$m). These trials using simulated beam data showed
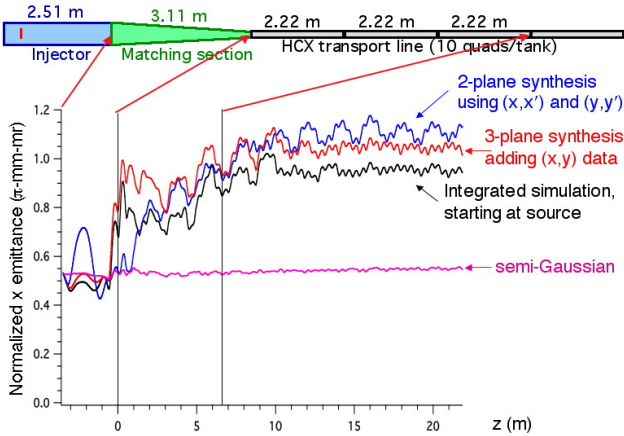
Figure 6: Simulation results: evolution of (x, x') emittance for self-consistent, 2-plane reconstruction, 3-plane reconstruction, and semi-Gaussian beams.

that a major improvement in fidelity may be achieved by replacing the traditional idealized initial beam with a synthesized distribution based on slit scan data, at least in cases

wherein the beam is not overly distorted.[11, 12]

We are beginning to employ such synthesis techniques to launch simulations with initial conditions developed from experimental data. Using an initial particle set generated from two measured views of the HCX beam, we ran a WARP simulation through the (2.22 m, 10 quad) transport line; see also [26]. In Fig. 7 we show the measured beam at the downstream station "D-end" and the corresponding simulation results. While the beam dimensions and some important features such as the "hollowing" in the spatial density show rough agreement, and the absence of some features in the simulated beam can be explained by the fact that it was loaded in the center of the pipe while the experimental beam had shifted off-center, the agreement between the simulated and measured beams is less than ideal.
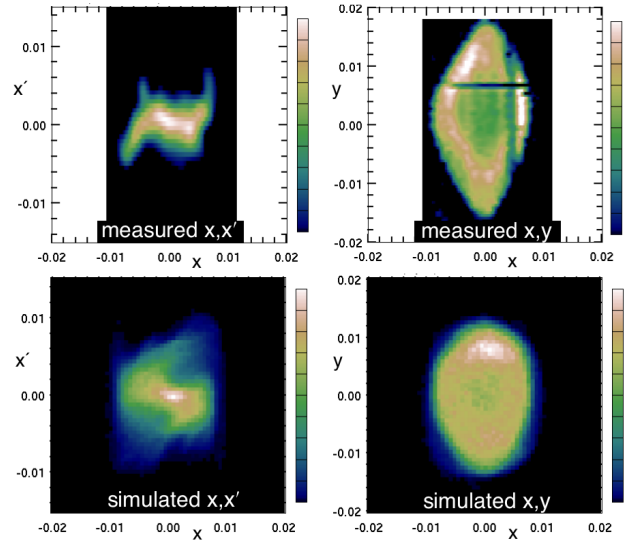
Figure 7: Top row: Experimentally measured (x, y) and (x, x') views of HCX beam at downstream station "D-end" (dark lines in latter are due to support wires); bottom row: simulation result, same views.

It was conjectured that correlations in unmeasured planes, *e.g.* (x', y), were not being captured by the synthesis process. This gave increased impetus to the development of new diagnostics that could yield projections such as $f(x, y, x')$. To this end, diagnostic slits moved by stepper motors were combined with scintillator-based imaging methods [27]. These "optical slit" methods indeed yield 3D (projectional) phase space information, but with relatively coarse sampling. As an example, the left panel of Fig. 8 shows $f(x', y)$, a "non-standard" projection of the 4D phase space density; the dark line traces the mean $x'(x=0)$ as a function of y, indicating an unanticipated correlation. In the right panel a rendering of the isosurface in 3D on which f is 30% of its peak value is shown; the thickening at the edge is indicative of an aberration in the beam-

confining lenses. Most recently, the Neutralized Transport Experiment (NTX) [28] is being diagnosed using an "optical hole plate" that can directly yield information about $f(x, y, x', y')$.
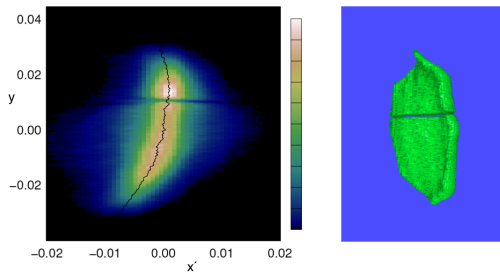

Figure 8: Experimentally measured projection $f(x', y)$ for HCX beam at station D-end using "optical slit" diagnostic, and 3D rendering of the 30% isosurface.

VI. OTHER DEVELOPMENTS

This paper has presented only a non-random sampling of the progress that is being made in the development of a quantitative, predictive understanding of the intense-beam physics needed for Heavy Ion Fusion, emphasizing studies of the beams in the driver accelerator itself. Comparable progress in simulating beam pulse compression [29] and transport through the fusion chamber [5, 28, 30, 31] has been made. Models of electron cloud effects in ion accelerators are being developed, and constraints on the allowable electron density in HIF drivers (due to deflections and instabilities) are being established [32, 33]. Future integrated experiments are also being developed with the aid of advanced simulations [34]. Descriptions of most of these topics can be found in these *Proceedings*.

ACKNOWLEDGEMENTS

REFERENCES

1 B. G. LOGAN, *et. al.*, these *Proceedings*.

2 C. M. CELATA, *et. al.*, *Phys. Plasmas* **10**, 2064 (2003).

3 A. FRIEDMAN, *AIP Conf. Proc.* **647**, 106 (2002).

4 D. P. GROTE, A. FRIEDMAN, G. D. CRAIG, I. HABER, and W. M. SHARP, *Nucl. Instr. and Meth.* **A 464**, 563 (2001).

5 D. R. WELCH, *et. al.*, these *Proceedings*.

6 H. QIN, *Phys. Plasmas* **10**, 2078 (2003).

7 E. SONNENDRUCKER, J. J. BARNARD, A. FRIEDMAN, D. P. GROTE, AND S. M. LUND, *Nucl. Instr. and Meth.* **A 464**, 470 (2001).

8 D. A. CALLAHAN, *et. al.*, these *Proceedings*.

9 G. WESTENSKOW, *et. al.*, these *Proceedings*.

10 P. A. SEIDL, *et. al.*, these *Proceedings*.

11 A. FRIEDMAN, D. P. GROTE, C. M. CELATA, and J. W. STAPLES, *Laser and Particle Beams* **21**, 17 (2003).

12 A. FRIEDMAN, D. P. GROTE, F. M. BIENIOSEK, C. M. CELATA, L. R. PROST, and P. A. SEIDL, *Proc. 2003 Particle Accel. Conf.* (2003).

13 J.-L. VAY, P. COLELLA, P. McCORQUODALE, B. VAN STRAALEN, A. FRIEDMAN, and D. P. GROTE, *Laser and Particle Beams* **20**, 569-575 (2002).

14 http://seesar.lbl.gov/ANAG/chombo/

15 D. P. GROTE, E. HENESTROZA, and J. W. KWAN, *Phys. Rev. Special Topics–Accel. and Beams* **6**, 014202 (2003).

16 C. BURKHART, J-L. VAY, P. A. SEIDL, and W. WALDRON, private communication, 2003.

17 R. C. DAVIDSON and H. QIN, *Physics of Intense Charged Particle Beams in High Energy Accelerators* (World Scientific, Singapore, 2001).

18 H. QIN, R. C. DAVIDSON, E. A. STARTSEV and W. W. LEE, *Laser and Particle Beams* **21**, 21 (2003).

19 A. FRIEDMAN, D. P. GROTE, and I. HABER, *Phys. Fluids* **B 4**, 2203 (1992).

20 I. HABER, A. FRIEDMAN, D. P. GROTE, S. M. LUND, and R. A. KISHEK, *Phys. Plasmas* **6**, 2254 (1999).

21 E. G. HARRIS, *Phys. Rev. Lett.* **2**, 34 (1959).

22 E. A. STARTSEV, R. C. DAVIDSON and H. QIN, *Phys. Plasmas* **9**, 3138 (2002).

23 E. A. STARTSEV, R. C. DAVIDSON and H. QIN, *Laser and Particle Beams* **20**, 585 (2002).

24 E. A. STARTSEV, R. C. DAVIDSON and H. QIN, *Phys. Rev. Special Topics–Accel. and Beams* **6**, 084401 (2003).

25 C. M. CELATA, A. FRIEDMAN, D. P. GROTE, I. HABER, E. HENESTROZA, *et. al.*, *Laser and Particle Beams* **20**, 577 (2002).

26 C. M. CELATA, *et. al.*, *Proceedings 2003 Particle Accel. Conf.*.

27 F. M. BIENIOSEK, L. R. PROST, and W. GHIORSO, *Proc. 2003 Particle Accel. Conf.*, paper wppb050 (2003).

28 E. HENESTROZA, *et. al.*, these *Proceedings*.

29 H. QIN and R. C. DAVIDSON, *Phys. Rev. Special Topics– Accel. and Beams* **5**, 034401 (2002)

30 W. M. SHARP, *et. al.*, these *Proceedings*.

31 S. S. YU, *et. al.*, these *Proceedings*.

32 A. W. MOLVIK, *et. al.*, these *Proceedings*.

33 P. A. STOLTZ, M. A. FURMAN, J-L. VAY, A. W. MOLVIK, and R. H. COHEN, *Phys. Rev. Special Topics–Accel. and Beams* **6**, 054701 (2003).

34 C. M. CELATA, *et. al.*, these *Proceedings*.